IAOS

International Association for Obsidian Studies

Bulletin

ISSN: 2310-5097

Number 76 **Summer 2026**

CONTENTS

NEWS AND INFORMATION

NEWS AND NOTES

Have news or announcements to share? Send them to IAOS.Editor@gmail.com for inclusion in the next issue of the *IAOS Bulletin.*

CONSIDER PUBLISHING IN THE IAOS *BULLETIN*

The *Bulletin* is a twice-yearly publication that reaches a wide audience in the obsidian community. Please review your research notes and consider submitting an article, research update, news, or lab report for publication in the *IAOS Bulletin*. Articles and inquiries can be sent to IAOS.Editor@gmail.com Thank you for your help and support!

Mark Your Calendar for the International Obsidian Conference 2026

From Magma to Artifact: The Geology and Archaeology of Obsidian
Yerevan, Armenia, 28 September – 01 October, 2026

Registration is now open!

See the flyer at the end of this issue of the *IAOS Bulletin*

https://ioc2026.geology.am/

NOTES FROM THE PRESIDENT

What feels like almost a lifetime ago marks the beginning of my serious involvement with obsidian research. I have been fascinated by this striking raw material ever since my first encounter with obsidian stone tools in museum exhibitions as a school student — and later, as an undergraduate archaeology student, handling obsidian fragments collected from the soil or sieve during summers spent excavating in Greece. The deeper my involvement with the material grew, the more captivated I became.

My Master's and subsequent PhD research only deepened my fascination with obsidian's unique aesthetic qualities, and this deep-rooted passion remains as strong as ever with each new research project I undertake. The culmination of these years dedicated to obsidian studies is the volume *Obsidian and the Sea: Evidence, Concepts and Social Implications of its Maritime Transportation*, which I edited alongside Dr. Christian Reepmeyer. Further details on the book's table of contents and how to access it can be found in the next section of the Bulletin.

Many of us will be presenting on topics addressed in the book at the forthcoming International Obsidian Conference in Armenia (IOC-2026). With abstract submissions and evaluations now concluded, preparations are well under way for what promises to be an exciting programme of talks, museum visits, and field trips — including to some truly impressive obsidian sources! Online registration and secure payment will be available soon on the conference website (https://ioc2026.geology.am), so keep an eye out if you plan to attend. Please see the updated circular at the end of this issue of the *IAOS Bulletin.*

Earlier this year, the IAOS held its annual board meeting at the SAAs in San Francisco. A range of topics were discussed, including future IAOS involvement in conferences, ongoing sponsorships, awards, and travel grants. I would also like to take this opportunity to remind everyone to renew their membership, as this directly enables us to continue supporting obsidian researchers worldwide.

We are also still seeking candidates for the positions of Secretary/Treasurer and Webmaster. If you or someone you know might be interested in either role, please don't hesitate to get in touch! The same applies to contributions to the Bulletin — have you recently given a talk, presented a poster, or published an article on an obsidian-related topic? We'd love to feature your work. You can submit contributions to Carolyn Dillian at IAOS.Editor@gmail.com.

Finally, we are delighted to announce our sleek new website! Take a virtual tour here: https://sites.google.com/obsidianstudies.com/iaos/home

On that note, summer is here and I trust many of you are already out in the field for some long-awaited geo-archaeological fieldwork. Good luck to all, and happy exploring!

Dora Moutsiou
Special Scientist
Archaeological Research Unit
University of Cyprus

NEW BOOK ALERT!

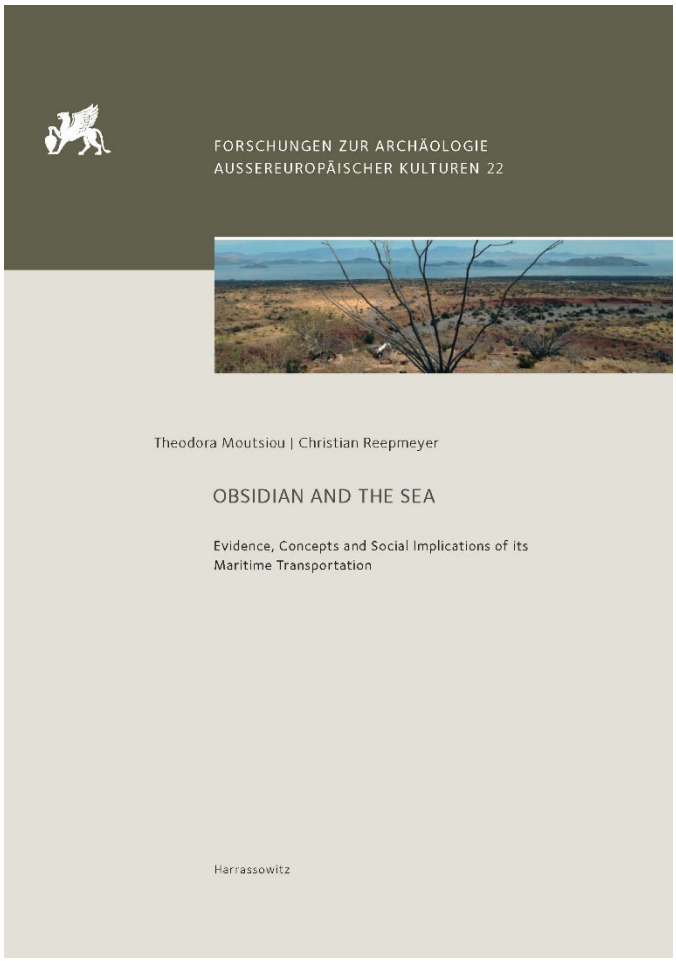

Theodora Moutsiou and Christian Reepmeyer

Obsidian and the Sea: Evidence Concepts and Social Implications of its Maritime Transportation

ISBN 9783447125277

For open access:
https://publications.dainst.org/books/dai/catalog/book/2180

To purchase:
https://www.harrassowitz-verlag.de/Obsidian_and_the_Sea/titel_9182.ahtml

Maritime exchange and its social dimensions substantially define global relationships in our modern world. Archaeology as a discipline has a long history investigating exchange and this research has been used to understand the extent of spheres of interactions between distant communities, risk minimisation strategies of communities living in unpredictable environments, advances in technology, cultural diversification, and emergence of social hierarchies and inequalities. This volume elucidates the long-lasting human relationship with the sea, demonstrating the crucial role of the coast and open waters alike in the development of prehistoric coastal communities, human migration trajectories and island settlement in deep time. This book's novel approach is to focus on one material in particular, obsidian, to explore how it reveals the use of the sea in prehistory across different times and places. The case studies presented here demonstrate especially well that humans throughout history and across different regions have engaged with obsidian exchange not solely as an economic activity but, significantly, in a symbolic way to denote social connectivity at great distances and oftentimes in absentia, meaning without the need for face-to-face interactions. Obsidian's unique physical attributes – brilliance, iridescence, transparency, colour – an integral part of the human condition with a strong emotional impact to its consumers, facilitated the maintenance of mental maps of preferential routes and desired social networks diachronically with the sea functioning as a highway for communication.

Obsidian and the Sea: Table of Contents

THE JAPANESE OBSIDIAN DATABASE: A WEBSITE PROVIDING COMPREHENSIVE SUPPORT FOR OBSIDIAN PROVENANCE ANALYSIS IN ARCHAEOLOGY

Yoshimitsu Suda[a] and Nobuyuki Ikeya[b]

[a] Faculty of Education, Nagasaki University, Japan
[b] Center for Obsidian and Lithic Studies, Meiji University, Japan

Introduction

Advances in analytical techniques since the 1970s, particularly X-ray fluorescence (XRF) analysis, have greatly enhanced the provenance analysis of archaeological obsidian in Japan and advanced our understanding of exchange networks and human mobility during the Palaeolithic and Jomon periods.

Approximately 80 obsidian sources exist in the Japanese archipelago (Figure 1), and vast numbers of obsidian artefacts have been recovered from Palaeolithic and Jomon archaeological sites. Despite the need for provenance analysis, several million unanalysed artefacts are currently stored in Japanese cultural heritage institutions, with several tens of thousands of new artefacts being discovered each year. This has become a significant problem in Japanese archaeology and in cultural heritage administration.

The number of institutions and laboratories capable of performing provenance analysis is limited, likely fewer than ten, even

Figure 1. Localities of geological obsidian samples curated at Nagasaki University and Meiji University

when private companies are included. Consequently, there is insufficient analytical capacity to meet the demand for provenance analysis. These issues could be addressed by expanding analytical facilities, particularly within cultural heritage institutions across Japan. To achieve this, our research is structured around the following three main pillars.

1. The development of non-destructive quantitative analysis of obsidian artefacts using energy-dispersive XRF (EDXRF), including the establishment of obsidian calibration standards based on Japanese obsidian.
2. The determination of discriminant (compositional) groups used in obsidian provenance analysis and associated reference obsidian specimens.
3. The development of data-processing algorithms and interfaces for performing obsidian provenance analysis.

Through these efforts, it is intended to establish a comprehensive framework for obsidian provenance analysis. The Japanese Obsidian Database: (https://sites.google.com/view/obsidian) serves as a key platform for facilitating the expansion of analytical facilities across Japan, providing a web-based interface for the provenance analysis of archaeological obsidian.

Principles of Obsidian Provenance Analysis

The workflow for obsidian provenance analysis is shown in Figure 2. Obsidian is a glassy volcanic rock that forms by the rapid cooling of high-silica (typically rhyolitic) magma. The chemical composition of magma varies, even among rhyolitic magmas, depending on the generation conditions (e.g., partial melting and fractional crystallisation) and ascent to shallow crustal levels. Consequently, the chemical composition of obsidian varies between volcanoes and

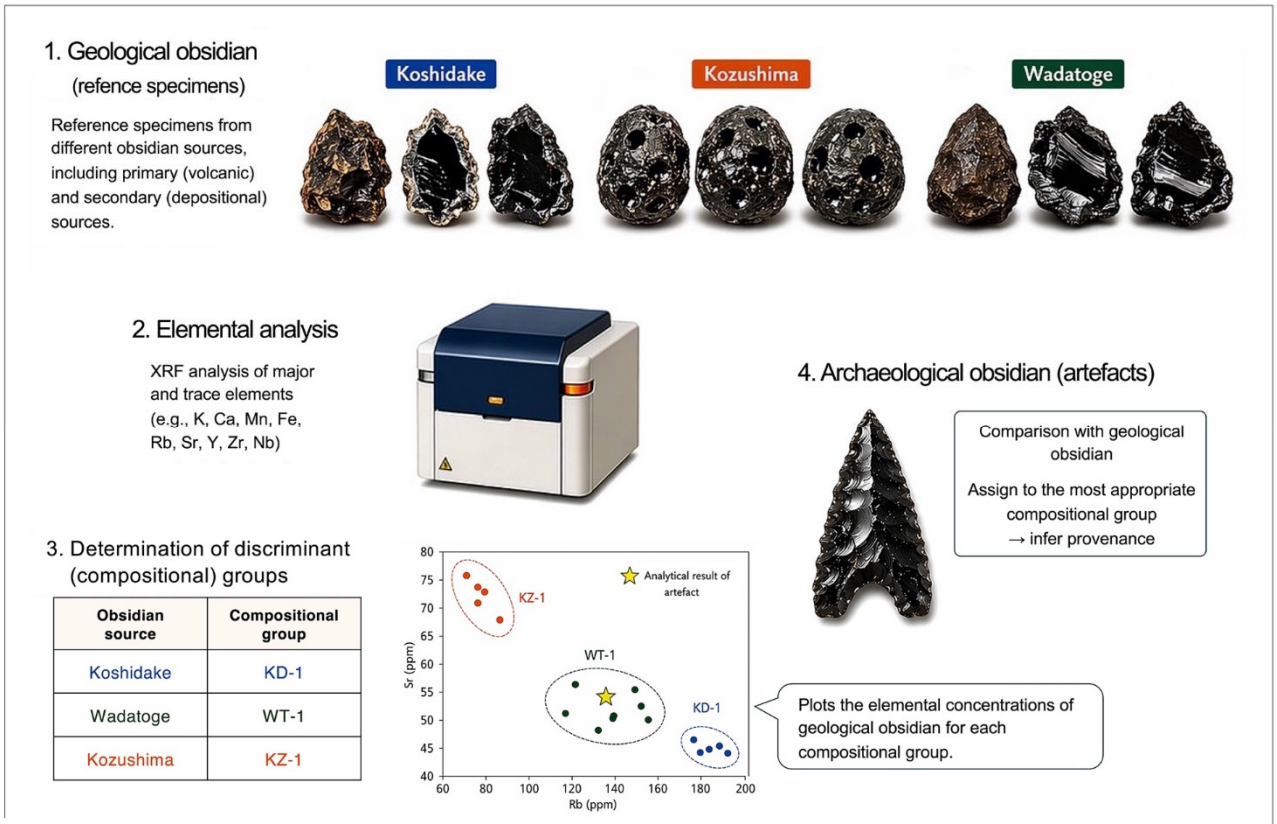

Figure 2. Workflow for obsidian provenance analysis.

between eruptions, allowing provenance to be determined.

In geology, an obsidian source is defined as a locality where obsidian was originally formed (i.e., the primary source). In contrast, in archaeology, an obsidian source refers to a location where obsidian was procured as a lithic raw material; therefore, this includes not only primary sources but also secondary deposits formed by fluvial transport (secondary sources).

Obsidian with identical chemical compositions may occur in primary and secondary sources that are separated by tens of kilometres or more and may also occur in multiple secondary sources. Furthermore, secondary sources may contain obsidian derived from multiple primary sources. In some cases, these include obsidian for which the geological source cannot be identified. Accordingly, it should be noted that compositional analysis (e.g., XRF) can only enable the assignment of discriminant (compositional) groups defined by the geochemistry of geological obsidian and cannot identify procurement locations directly.

To identify the procurement locations of obsidian through provenance analysis, additional steps beyond compositional analysis are required. These include examining the geographical distribution of obsidian for each compositional group, as well as its physical characteristics, including surface features (patina), morphology (e.g., rounded or angular shapes), and size. The Japanese Obsidian Database provides information on the geographic distribution of obsidian in each compositional group. In addition, obsidian sources are classified as either primary or secondary.

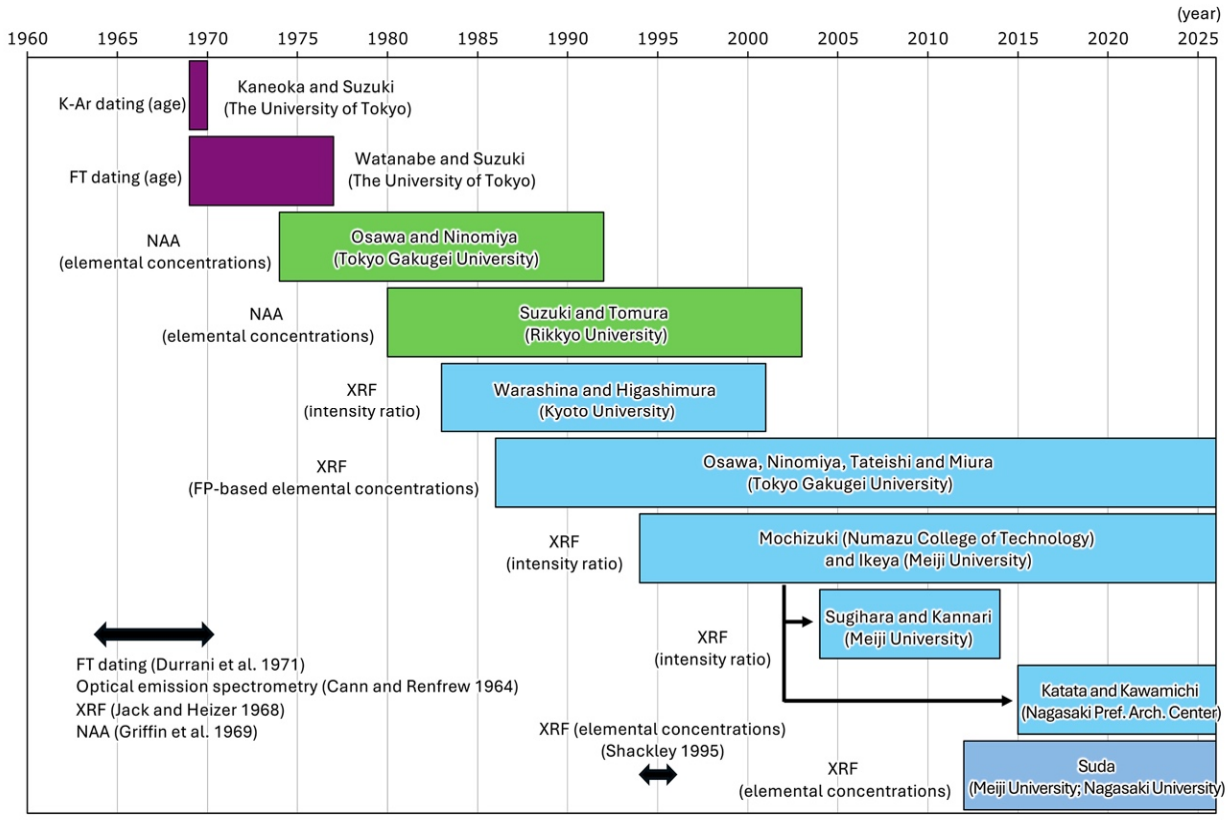

Figure 3. Timeline of the analytical methods used for obsidian provenance studies.

History of Analytical Techniques Used for Obsidian Provenance Analysis in Japan

Figure 3 provides a summary of the history of the analytical techniques used for obsidian provenance analysis in Japan. Instrumental approaches to obsidian provenance analysis began in the late 1960s with a research group at the University of Tokyo (Kaneoka 1969; Kaneoka and Suzuki 1970; Watanabe and Suzuki 1969). These early studies were based on chronometric techniques, including K–Ar and fission-track (FT) dating. At that time, K–Ar dating had not been established as a practical method for provenance analysis, whereas FT dating was used in combination with hydration dating (Tsurumaru et al. 1973).

Provenance analysis using neutron activation analysis (NAA) was conducted during the 1970s by research groups at Tokyo Gakugei University (Osawa 1974) and Rikkyo University (Suzuki and Tomura 1983), using a research reactor at Rikkyo University. This method enabled the analysis of trace element contents in geological and archaeological obsidian at ppm levels, and systematic obsidian provenance analysis was conducted widely in Japan until the shutdown of the research reactor in 2001.

During the 1980s, EDXRF began to be used for obsidian provenance analysis by a research group at Kyoto University (Warashina and Higashimura 1983), and subsequently by a research group at Tokyo Gakugei University (Ueno et al. 1986; Daikuhara et al. 2024; Fujimori et al. 2026). The introduction of EDXRF greatly advanced obsidian provenance analysis in Japan; however, unlike NAA, this approach did not provide elemental concentrations in ppm. Intensity ratios were used at Kyoto University, and FP-based (standardless) elemental concentrations were employed at Tokyo Gakugei University, meaning that data could not be compared directly between different studies and laboratories.

During the 1990s, Akihiko Mochizuki and Nobuyuki Ikeya established a method for obsidian provenance analysis using EDXRF (Mochizuki et al. 1994) and established highly effective discrimination diagrams that are applicable across the Japanese archipelago. Despite the continued reliance on intensity

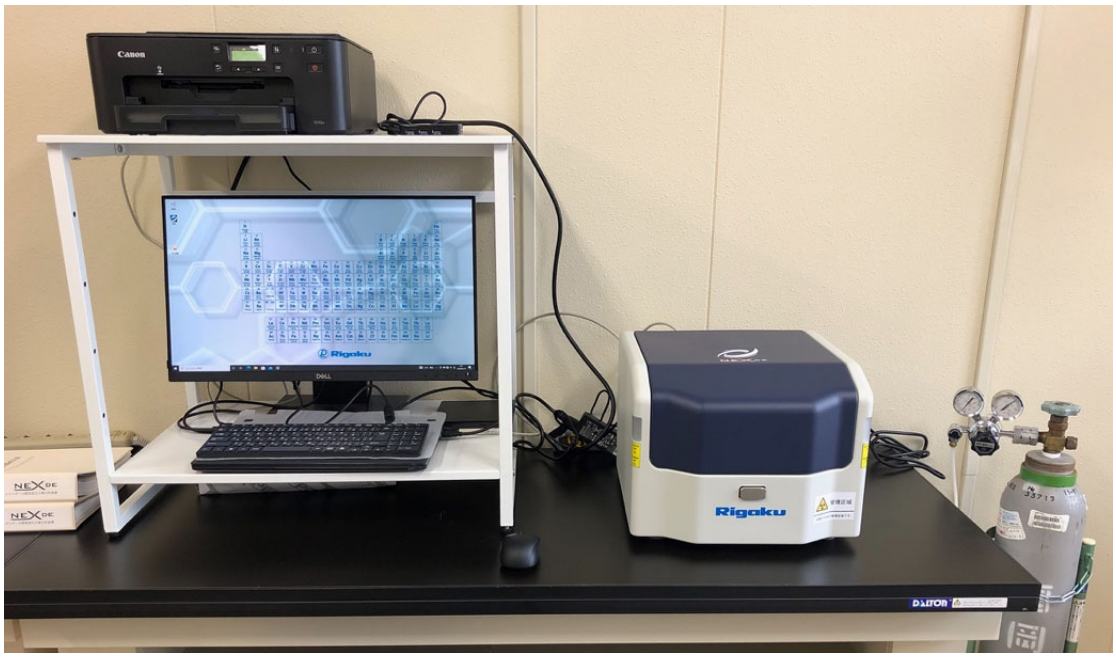

Figure 4. EDXRF instrument (Rigaku NEX DE) installed at Nagasaki University

ratios and fractions (rather than elemental concentrations), obsidian provenance analysis began to be conducted at several institutions across Japan. For example, analytical facilities have been established since the 2000s at Meiji University (Sugihara and Suzuki 2005; Kannari 2014) and the Nagasaki Prefectural Archaeological Center (Katata 2015; Kawamichi et al. 2017). This method is now the standard approach for obsidian provenance analysis in Japanese archaeology.

Although this method is applied widely in Japanese archaeology, the issues regarding direct comparison between studies and laboratories remains unresolved. This is particularly problematic in regional archaeological studies; for example, between the Korean Peninsula and Kyushu, Hokkaido and Sakhalin, and between Taiwan and the Ryukyu Islands. Therefore, provenance analysis based on elemental concentrations (ppm or wt.%) is required, especially in an international context.

A method for obsidian provenance analysis using quantitative EDXRF data (i.e., elemental concentrations) was developed around 1995 at the University of California, Berkeley (e.g., Shackley 1995). Subsequently, Yoshimitsu Suda (Meiji University, 2011–2013; Nagasaki University, 2014–) began developing provenance analysis using quantitative XRF data (Suda 2014). In 2023, EDXRF instruments (Rigaku NEX DE) were installed at Meiji University and Nagasaki University (Figure 4), and efforts were made to promote quantitative EDXRF-based provenance analysis.

Previous studies have shown that the K, Ca, Mn, Fe, Rb, Sr, Y, Zr, and Nb concentrations of obsidian are effective for discriminating between different lava flows and volcanoes across the Japanese archipelago (e.g., Suda et al. 2021). Therefore, a quantitative EDXRF method for the non-destructive analysis of archaeological obsidian is being developed for these elements (e.g., Suda et al. 2025).

Establishment of Obsidian Calibration Standards and a Quantitative EDXRF Analytical Framework

A major challenge in quantitative EDXRF-based provenance analysis is achieving reliable non-destructive analysis of archaeological obsidian. Archaeological obsidian is subject to greater analytical constraints than geological obsidian. For geological obsidian, there are essentially no restrictions on sample preparation; measurement surfaces can be flattened, and high-precision analysis using wavelength-dispersive X-ray fluorescence (WDXRF) on fused glass beads can be performed when necessary. In WDXRF analysis using fused glass beads, powdered rock standards provided by the US National Institute of Standards and Technology (NIST) and the Japanese National Institute of Advanced Industrial Science and Technology (AIST) can be used. In contrast, the analysis of archaeological obsidian must be strictly non-destructive. Given these constraints, quantitative EDXRF analysis of archaeological obsidian requires corrections for geometry as well as for matrix effects and spectral interference. Furthermore, the preparation of solid calibration standards is essential.

Solid obsidian standards have been developed by Yale University (PYRO; Frahm 2019) and the University of Missouri Research Reactor (MURR; Glascock 2020). The MURR standards provide reference values for the elements required for our analyses (K, Ca, Mn, Fe, Rb, Sr, Y, Zr, and Nb), whereas the PYRO standards do not cover all of these elements. In addition, it is desirable to use standards composed primarily of Japanese obsidian for analysing archaeological obsidian from Japan; therefore, we developed a new obsidian

Figure 5. Calibration standards: the Japanese Obsidian Standards (JOS).

calibration standard set using 39 geological obsidian samples from Japan and several other countries (Figure 5).

We refer to this set as the Japanese Obsidian Standards (JOS), and the reference values for this standard set were determined using WDXRF on fused glass beads with a Rigaku Primus III+ at Meiji University (Figure 6). These reference values include concentrations of major elements (SiO_2, TiO_2, Al_2O_3, Fe_2O_3t, MnO, MgO, CaO, Na_2O, K_2O, and P_2O_5) and trace elements (Zn, Rb, Sr, Y, Zr, Nb, and Th). The sample localities and reference values are provided in the Japanese Obsidian Database.

To enable the practical use of these obsidian standards, we are currently developing an application package (Obsidian Application Pack) for use with a Rigaku EDXRF instrument (NEX DE). In practice, quantitative analysis following instrument installation requires several preparatory steps, including the optimisation of measurement conditions, the measurement of standard samples, and construction of calibration curves. These procedures pose significant challenges, particularly for staff working in cultural heritage institutions. This application package can eliminate these steps and provide an environment in which the quantitative analysis of obsidian can begin immediately after instrument installation.

This application package includes calibration curves for K, Ca, Mn, Fe, Zn, Rb, Sr, Y, Zr, and Nb based on the Japanese Obsidian Standards. Corrections for matrix effects, spectral interference, and geometric variations using the Compton scatter internal standard method are incorporated, enabling the non-destructive quantitative analysis of archaeological obsidian. The measurement area is 3 mm in diameter. Three measurement-time modes (5.0, 3.5, and 2.5 min) are provided. For the analysis of archaeological obsidian, the 2.5 min mode is typically used. In addition, obsidian from Koshidake (northwestern Kyushu) is recommended for use in drift calibration and quality control.

Reference Obsidian Specimens and Assignment of Discriminant Groups Based on Quantitative Data

The determination of discriminant

Figure 6. WDXRF instrument (Rigaku Primus III+) installed at Meiji University (Center for Obsidian and Lithic Studies, Nagano).

(compositional) groups based on compositional analysis of geological obsidian is crucial for provenance analysis of obsidian artefacts (Figure 2). In our laboratory, geological obsidian collected from each source is first prepared by polishing a flat surface using #600 grit carborundum for EDXRF analysis. Several scatter plots based on elemental concentrations, elemental ratios, and elemental fractions are constructed for each source. Compositional groups are identified based on clustering patterns observed in these plots. Samples falling within ±3σ of the mean elemental composition of each cluster are assigned to the same compositional group.

To evaluate the validity of these groups, more than ten samples from each group are selected and analysed using WDXRF by the fusion bead method at Meiji University (Figure 6). In this WDXRF analysis, concentrations of major (SiO_2, TiO_2, Al_2O_3, Fe_2O_3t, MnO, MgO, CaO, Na_2O, K_2O, and P_2O_5) and trace elements (Zn, Rb, Sr, Y, Zr, Nb, and Th) are determined (Suda and Ikeya 2021). If further subdivision of compositional groups is indicated by the WDXRF data, the groups are refined accordingly. The compositional groups defined through this process are then compared with those defined for other sources based on WDXRF data to assess potential overlap or compositional equivalence. In cases where compositional equivalence is indicated, the groups are treated as a single compositional group.

We define the reference obsidian specimens for each discriminant group, consisting of 12 obsidian discs with diameters of 1–3 cm, polished with #600 grit carborundum and stored in plastic cases (Figure 7). Using these reference obsidian specimens, we develop an algorithm for the provenance analysis of archaeological obsidian, as described below.

The analysis is performed based on the following four diagrams:

1: 100 × Rb/(Rb + Sr + Y + Zr) versus 100 × Sr/(Rb + Sr + Y + Zr),
2: 100 × Sr/(Rb + Sr + Y + Zr) versus ln(100 × Fe/K),
3: 100 × Rb/(Rb + Sr + Y + Zr) versus ln(100 × Mn/Fe), and
4: 100 × Zr/(Rb + Sr + Y + Zr) versus ln(100 × K/Ca).

Figure 7. Reference obsidian specimens from northwestern Kyushu.

Discriminant ellipses are then constructed for each discriminant group in these diagrams. Twelve reference obsidian specimens from each discriminant group were analysed, and each specimen was measured twice, yielding a total of 24 data points. Analytical data points were screened for outliers, and those containing values beyond ±3σ of the mean were excluded. Rotated ellipses were subsequently constructed from the remaining data using principal component analysis (PCA), with ellipse boundaries defined as ±3σ of the data distribution, following Suda and Namba (2026).

Confidence ellipses are often used in provenance analysis (e.g., Glascock 2020). However, confidence ellipses are based on the assumption that the variables follow a multivariate normal distribution. In our approach, elemental ratios and fractions are used, and their distributions do not necessarily satisfy this assumption. Therefore, the use of confidence ellipses is not appropriate.

Finally, we plot the compositional data of archaeological obsidian obtained by EDXRF analysis. Group assignment is considered valid only when a sample falls within the ellipses of the same discriminant group across all four diagrams; otherwise, the result is deemed inconclusive. Figure 8 shows the four diagrams, each with discriminant ellipses constructed from geological obsidian in northwestern Kyushu.

Conclusion

Our goal is not to create a monopolistic framework for obsidian provenance analysis, but to establish a framework that can be readily implemented by other institutions. To this end, we are developing an obsidian analysis application package for EDXRF, establishing reference obsidian specimens, and creating data processing algorithms together with web-based interfaces to reduce the technical barriers to conducting obsidian provenance analysis using EDXRF.

The Japanese Obsidian Database provides information on obsidian discriminant groups across the Japanese archipelago, together with their geographic distribution and representative compositions determined by WDXRF. In addition, the Japanese Obsidian Standards and the reference obsidian specimens presented in

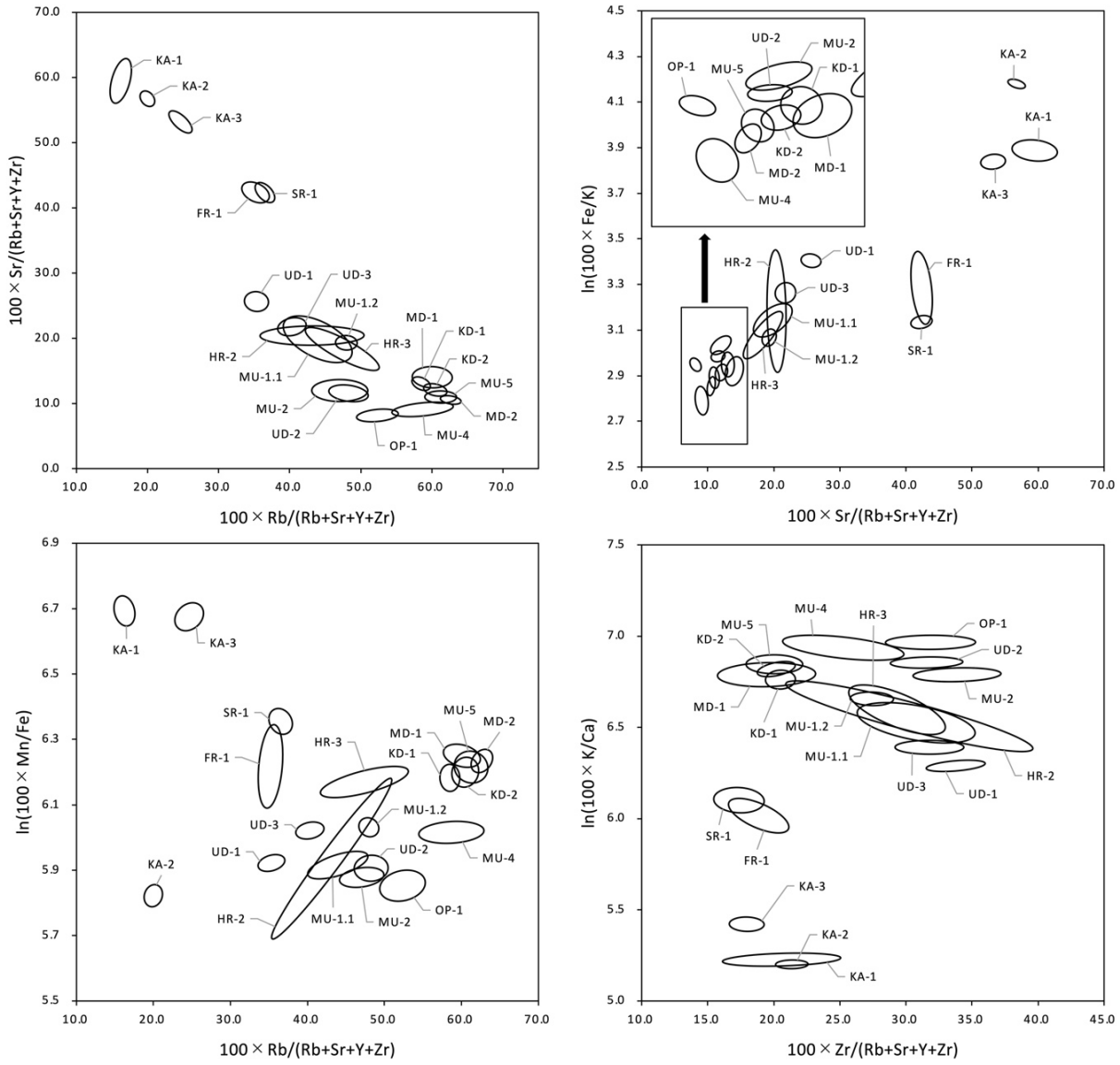

Figure 8. Diagrams used to assign discriminant (compositional) groups in obsidian provenance analysis. Discriminant ellipses for each group are constructed from geological obsidian in northwestern Kyushu: KD-1 (Koshidake and Hoshika Peninsula), KD-2 (Kurokamiyama), MD-1 and MD-2 (Osaki Peninsula and Mukyudo), MU-1.1, MU-1.2, MU-2, MU-4 and MU-5 (Hoshika Peninsula), OP-1 (Osaki Peninsula), KA-1, KA-2, and KA-3 (Kamedake and Ogushi), SR-1 (Shiibagawa), and UD-1, UD-2, HR-2, HR-3, and FR-1 (Hario Island). Parentheses indicate the obsidian sources. For details, see the Japanese Obsidian Database.

the database are available through a loan system in accordance with Nagasaki University regulations.

We continue to conduct fieldwork and XRF analyses to define additional discriminant groups across the Japanese archipelago and regularly update the database as our research progresses. Through these efforts, we aim to facilitate the broader adoption of obsidian provenance analysis in Japan and to strengthen the international obsidian research community.

References Cited

Cann, John R., and Colin Renfrew. 1964. The characterization of obsidian and its application to the Mediterranean region. *Proceedings of the Prehistoric Society* 30:111–133.

Daikuhara, Y., Masaru Miura, T. Tateishi, and Shigeki Ninomiya. 2024. Behavioural territories of Early Jomon people inferred from obsidian and arrowheads. *Quaternary Research* 65:2413–2428 (in Japanese).

Durrani, Shafique A., H. A. Khan, M. Taj, and Colin Renfrew. 1971. Obsidian source identification by fission track analysis. *Nature* 233:242–245.

Frahm, Ellery. 2019. Introducing the Peabody-Yale reference obsidian (PYRO) sets: Open-source calibration and evaluation standards for quantitative X-ray fluorescence analysis. *Journal of Archaeological Science: Reports* 27:101957.

Fujimori, Eiji, Kazumichi Serizawa, Nobuyuki Ikeya, and Takashi Tsutsumi. 2026. Dynamics of obsidian use during the latter half of the Middle Jomon period on the southern foothills of Mt. Asama—provenance analysis of obsidian artefacts from the Kawarada, Hirohata, and Omogae-koyagasawa site (Area A), Nagano, Japan. *Natural Resource Environment and Humans* 16:63–82 (in Japanese).

Glascock, Michael D. 2020. A systematic approach to geochemical sourcing of obsidian artifacts. *Scientific Culture* 6(2):35–47.

Griffin, James B., Adon A. Gordus, and Gordon A. Wright. 1969. Identification of the sources of Hopewellian obsidian in the Middle West. *American Antiquity* 34(1):1–14.

Jack, Robert N., and Robert F. Heizer. 1968. "Finger-printing" of some Mesoamerican obsidian artifacts. *Contributions of the University of California Archaeological Research Facility* 5:81–100.

Kaneoka, Ichiro, and Masao Suzuki. 1970. K–Ar and fission track ages of some obsidians from Japan. *Journal of the Geological Society of Japan* 76:309–313.

Kannari, Taro. 2014. Provenance estimation results of obsidian artefacts (unpublished data from 2010–2013). *Natural Resource Environment and Humans* 4:99–104 (in Japanese).

Katata, Masaki. 2015. Provenance estimation of obsidian using a discriminant diagram method: Accumulation of source data. *Bulletin of the Nagasaki Prefectural Archaeological Center* 5:35–40 (in Japanese).

Kawamichi, Hiroshi, Masahiro Katata, and Naoto Tsujita. 2017. Advances in obsidian provenance studies in Nagasaki Prefecture: Analysis of lithic assemblages from the Harunotsuji site. *Bulletin of the Nagasaki Prefectural Archaeological Center* 7:21–40 (in Japanese).

Mochizuki, Akihiko, Nobuyuki Ikeya, Katsuji Kobayashi, and Yuri Muto. 1994. Provenance estimation and distribution of obsidian artefacts from archaeological sites in Shizuoka Prefecture, Japan. *Shizuoka Archaeological Research* 26:1–20 (in Japanese).

Osawa, Masumi, Koji Ida, and Kunio Yoshida. 1974. Determination of major and trace elements in obsidian and jadeite by neutron activation analysis. *Bulletin of Tokyo Gakugei University, Natural Sciences* 26:187–207 (in Japanese).

Shackley, M. Steven. 1995. Sources of archaeological obsidian in the greater American Southwest: An update and quantitative analysis. *American Antiquity* 60(3):531–551.

Suda, Yoshimitsu. 2014. Application of internal standard method to non-destructive analysis of obsidian artifacts by wavelength dispersive X-ray fluorescence spectrometry. *BAR International Series* 2620:33–45.

Suda, Yoshimitsu, and Nobuyuki Ikeya. 2021. Precision, accuracy and quantitative analyses of geologic obsidian by WDXRF in the Center for Obsidian and Lithic Studies (COLS), Meiji University. *Natural Resource Environment and Humans* 11:1–23 (in Japanese).

Suda, Yoshimitsu, Tatsuro Adachi, Kazutaka Shimada, and Yasuhito Osanai. 2021. Archaeological significance and chemical characterization of the obsidian source in Kirigamine, central Japan: Methodology for provenance analysis of obsidian artefacts using XRF and LA-ICP-MS. *Journal of Archaeological Science* 129:105377.

Suda, Yoshimitsu, Kazutaka Shimada, Keiji Wada, Masayuki Mukai, Tetsuro Adachi, and Nobuyuki Ikeya. 2025. Non-destructive method of archaeological obsidian provenance analysis using EDXRF: A case study of obsidian in Hokkaido, northern Japan. *Journal of Archaeological Science: Reports* 66:105287.

Suda, Yoshimitsu, and Yui Namba. 2026. A methodology for provenance analysis of archaeological obsidian based on quantitative EDXRF: A case study of the Oki-Dogo and Iki Island sources, southwest Japan. *Natural Resource Environment and Humans* 16:23–41 (in Japanese).

Sugihara, Shigeo, and Masafumi Suzuki. 2005. Provenance estimation of Jomon-period obsidian artefacts from the Sannai-Maruyama site, Aomori Prefecture, Japan. *Special Historic Site Sannai-Maruyama Site Annual Report* 9:22–35 (in Japanese).

Suzuki, Masao, and Kenji Tomura. 1983. Basic data for identifying the source of archaeological obsidian by activation analysis and discriminant analysis. *St. Paul's Review of Science* 4(4):99–110.

Tsurumaru, Toshiaki, Shizuo Oda, Naoki Isshiki, and Masao Suzuki. 1973. Problems in the provenance estimation of obsidian from the Izu Islands. *Cultural Properties Conservation* 5:147–158 (in Japanese).

Ueno, Shuichi, Shuji Ninomiya, Mamoru Aboshi, and Masumi Osawa. 1986. Utilisation of obsidian in the Stone Age in Tochigi Prefecture, Japan. *Bulletin of the Tochigi Prefectural Museum* 3:91–115 (in Japanese).

Warashina, Tetsuo, and Takenobu Higashimura. 1983. Provenance analysis of lithic materials by X-ray fluorescence. *Journal of the Society for the Conservation of Cultural Property* 16(2):59–78 (in Japanese).

Watanabe, Naotune, and Masao Suzuki. 1969. Fission track dating of archaeological glass materials from Japan. *Nature* 222:1057–1058.

ACCURACY AND PRECISION OF ANALOG TEMPERATURE CELLS FOR OBSIDIAN HYDRATION DATING

Alexander K. Rogers[a] and Christopher M. Stevenson[b]

[a] Maturango Museum, Ridgecrest, California, USA
[b] Virginia Commonwealth University, Richmond, Virginia, USA

Abstract
We present a mathematical analysis of the calibration and use of analog temperature cells for measuring the effective hydration temperature (EHT) for obsidian hydration age determination. Although digital temperature cells are currently popular, analog cells are still in use by some archaeologists due to the lower cost. We find that the precision of analog cells in measuring the cell reaction temperature is approximately 0.3°C, but this reaction temperature is lower than the EHT for obsidian, with a 1 - 2°C offset. We also provide an adjustment to correct this offset, which will yield an obsidian EHT with a precision of approximately 1°C. Finally, we briefly summarize a dynamic EHT computation with digital temperature cells, which gives an uncertainty in EHT of within 0.5°C. The results of this study permits the recalculation of past obsidian hydration dates as greater levels of certainty.

Introduction

The hydration rate of obsidian is strongly temperature-dependent, so archaeological chronometrics by obsidian hydration dating (OHD) depend on a correct temperature assessment at an archaeological site. Analog cells were used to evaluate ground temperature prior to the development of digital cells and are still used in some applications. The primary analog cell used in the past was the Ambrose/Trembour cell, while the Pallmann cell was used less frequently. In analog cells a rapidly-progressing chemical or physical phenomenon was used as a proxy for the slower process of obsidian hydration, the key being that both followed an Arrhenius relationship with temperature. In this paper, we present a mathematical analysis of the calibration and use of analog cells, and quantify the accuracy and precision. We also provide an adjustment to improve accuracy in new OHD applications. Finally, we briefly summarize a dynamic method possible with digital temperature cells, which gives the best accuracy in EHT attainable at present.

Although digital cells are now popular, analog cells are still in use by some archaeologists, so this analysis is of more than antiquarian interest. Furthermore, the adjustment method we describe will be useful in interpreting previously published OHD age data that were based on analog cells.

Obsidian Hydration

Obsidian hydration is essentially a water absorption process (Doremus 2002; Stevenson et al. 2021). When a fresh surface of obsidian is exposed to air, water molecules adsorb onto the surface. Some of the adsorbed water molecules, plus other water molecules impinging directly from the atmosphere, diffuse into the Si-OH interstices within the glass matrix. Stevenson et al. (2021) provides a detailed description of the interaction of the adsorbed layer with the glass surface. Since the water is transported into the glass by diffusion, the water penetration depth (r) is directly proportional to the square root of time (t) (Crank 1975), which leads to an age equation of:

$$t = r^2/k \quad (1)$$

in which k is the hydration rate (Friedman and Smith 1960). The depth of water penetration is typically measured by optical microscopy although infrared spectroscopy is gaining in popularity (Franchetti et al. 2024).

For absorption to occur, a water molecule must have sufficient kinetic energy to stretch the glass matrix and enter one of the interstices. Because energy is proportional to temperature, the process is temperature-dependent and exponential in nature. The temperature dependence of the diffusion rate is described by the Arrhenius equation:

$$k = k_0 * \exp(-Q/T) \qquad (2)$$

where: k is the diffusion rate, k_0 is a constant, Q is activation energy in Kelvins (K), and T is temperature in Kelvin. For naturally occurring obsidians the value of Q lies between approximately 9000 K and 11000 K (Friedman and Long 1976; Trembour and Friedman 1984). Thus, the obsidian experiences water transport at a rate which varies with time, and the archeological hydration rate is the average of the instantaneous rate over the life of the artifact. This average rate (k_{arch}) can be expressed as an integral:

$$k_{arch} = (1/\tau)\int k_0 * \exp(-Q/T)dt \qquad (3)$$

where: τ is the time since the surface was exposed to water vapor (i.e., the archaeological age), and the integral is taken over zero to τ. Equation (3) has no analytic solution, but it can be solved as a finite sum:

$$k_{arch} = (1/N) * k_0 * \sum\exp[-Q/T(n)] \qquad (4)$$

where: T(n) is a time series of temperature data points and the sum is taken over N points which correspond to time τ. For archaeological computations the assumption is made the temperature is essentially stable year to year, so that performing the sum over one year is representative of the age of the artifact and typically the sampling rate is hourly.

By definition, the constant temperature value which yields k_{arch} is the effective hydration temperature (EHT), so

$$EHT = -Q/\ln\{\sum\exp[-Q/T(n)]\} \qquad (5)$$

In the discussion that follows, we use the more general term "effective reaction temperature" (ERT) for the analog cells and reserve the term EHT for obsidian hydration only.

The Ambrose/Trembour Cell

The Ambrose cell was proposed and developed by Wallace Ambrose (1975, 1980) and is based on water diffusion through a semi-permeable plastic membrane. A small cell of plastic was filled with desiccant and placed within a water jacket where it is exposed to ambient temperature at the archaeological site. The water diffused through the plastic into the cell at a rate determined by the Arrhenius equation, the gain in weight was measured, and the weight gain/unit time was related to the ERT. The Trembour cell was similar but worked in reverse: the cell was filled with water and surrounded by salt desiccant, and the weight loss was measured, but the principle was the same (Trembour et al. 1988).

The diffusion process for such a cell (described mathematically by Crank 1975: 44ff.) is described by the Arrhenius equation, so the weight gain per unit time (dw/dt) is:

$$dw/dt = A_c * \exp(-Q_c/T) \qquad (6)$$

where: A_c is a constant, Q_c is the activation energy for the diffusion process in K, and T is time-varying temperature in K. For the plastics used in the cells, the activation energy is typically in the range of 3,500 – 5,000 K (Trembour et al. 1988:379).

Before archaeological measurements can be made, the values of A_c and Q_c must be determined by calibration, typically of a batch

of cells. Cells are exposed to controlled temperatures in laboratory ovens for a measured period of time, and the weight gain (or loss) measured. The values of $\ln(A_c)$ and Q_c are then determined by the log-Arrhenius process (Rogers and Stevenson 2017). Subsequently, a linear least-squares best fit between ln(dw/dt) vs. 1/T gives $-Q_c$ as the slope and $\ln(A_c)$ as the y-intercept. For a commercially available polycarbonate cell, typical values are $\ln(A_c) \approx 18.00$ and $Q_c \approx 5404$ Kelvins (Trembour et al. 1988:379).

Once the calibration constants are known, the effective reaction temperature for the cell at a site is computed as:

$$ERT = Q_c/[\ln(A_c) - \ln(dw/dt)] \qquad (7)$$

where: dw/dt is the measured gain (or loss) in weight of the cell. A precision in ERT of 0.01°C to 0.1°C was claimed for such cells (Trembour et al. 1986: 187, Table 2).

Referring to equation (5), the effective reaction temperature for such a cell is explicitly related to temperature history by the equation:

$$ERT = -Q_c/\ln\{\sum\exp[-Q_c/T(n)]\} \qquad (8)$$

However, as we will show below, the ERT for the Ambrose/Trembour cell is not identical to the EHT for obsidian, even with the same temperature history.

The accuracy and precision achievable with an analog cell are determined by the accuracy with which weight gain (or loss) or optical axis rotation can be measured, the accuracy of the calibration constants used to convert the measurement to temperature, and the effects of the activation energy on the resulting ERT. We make a distinction between precision and accuracy, because the first two factors affect precision only, while the third causes an offset which affects accuracy as well.

Measurement

To evaluate the precision of the measurement process we used a simple Monte Carlo simulation of equation (7), using typical parameter values, assumed to be error-free (Q_c = 5412 K, $\ln(A_c)$ = 11.27). The time was assumed to be 365 days, yielding a weight gain of 0.3 grams. The measurement accuracy was assumed to be one milligram in mass (standard deviation) and ten minutes in time (upper and lower limits). The simulation ran for 10,000 iterations, and yielded a standard deviation of the ERT of 0.053°C, which is mid-range in the precision reported by Trembour et al. (1986: 187, Table 2). Thus 0.05°C is a reasonable estimate of uncertainty due to measurement.

Calibration

A critical assumption in the above simulation was that the calibration parameters

Cell No.	Time (days)	Wt. gain(gm)	Temperature (°C)
2002-61	32.97	0.0344	25
2002-62	32.97	0.0333	25
2002-63	32.97	0.0628	35
2002-64	32.97	0.0635	35
2003-1	32.22	0.0765	40
2003-2	32.22	0.0784	40
2003-3	32.22	0.0434	30
2003-4	32.22	0.0443	30
2003-57	64.10	0.0874	30
2003-58	64.10	0.0892	30

Table 1. Ambrose cell parameters.

were error-free, which we know is not the case in the real world. To estimate the uncertainties of the calibration we used an unpublished data set by one of the authors (CMS), Table 1.

The parameter values for Q_c and $\ln(A_c)$ can be found by a linear least square best fit between ln(wt. gain/unit time) and 1/T, with T in Kelvins and the least squares analysis will also yield the uncertainties in both Q_c and $\ln(A_c)$. However, the errors are strongly correlated, so evaluating the effect of these errors on ERT cannot be performed analytically but requires a Monte Carlo simulation. The data set of Table 1 was used as the basis, with uncertainties of one milligram in mass and ten minutes in time. Again, 10,000 iterations were used. The resulting parameter values are $Q_c = 5416 \pm 124$ Kelvins and $\ln(A_c) = 11.29 \pm 0.40$. The uncertainties in the parameters lead to root-mean-square (rms) residuals in ERT of 0.295°C, which adds to the uncertainty due to measurement errors alone (0.053°C, above). Thus, the overall precision of the effective reaction temperature experienced by an Ambrose/Trembour cell is approximately 0.3°C.

Activation Energy Effects

The equation for ERT, equation (5) above, clearly shows that ERT is dependent on activation energy, in both numerator and denominator. Activation energy for obsidian hydration is about 10,000 K, while activation energy for diffusion in the cell is about 5,000 K. By equation (8) the EHT for an obsidian specimen at a site is:

$$EHT_o = -Q_o / \ln\{\sum \exp[-Q_o/T(n)]\} \quad (9)$$

while an Ambrose/Trembour cell under the same archaeological site conditions would yield an effective reaction temperature of:

$$ERT_c = -Q_c / \ln\{\sum \exp[-Q_c/T(n)]\} \quad (10)$$

The time series T(n) is the same in both cases, but there is no way to separate the Q from the Q/T term in the sum of the exponentials. Furthermore, the temperature history T(n) depends on three parameters: annual mean temperature; seasonal variation of the mean; and diurnal variation. The approach we used to evaluate the difference between ETH_o and ERT_c was another Monte Carlo simulation which computed effective temperature from equation (5) by numerical integration over a temperature history model, using activation energies for both the cell and for obsidian. A wide variety of temperature parameter values were used which bracket the temperatures of archaeological interest, and the results averaged. For each set of temperature parameters, the code computed EHT and ERT by equations (9) and (10) were computed, and the difference between them evaluated. The number of iterations was 10,000. The result was that the EHT experienced by the obsidian was 1.616 ± 0.558°C higher than the ERT experienced by the cell. Furthermore, out of 10,000 iterations, the ERT of the cell was never greater than the EHT of the obsidian. Thus, not taking activation energy into account underestimates the EHT, so both accuracy and precision are affected.

Adjustment Method

Since the offset due to activation energy differences are systematic, it is possible to adjust the ERT of a cell to represent the EHT of obsidian. The adjustment requires measuring (or inferring from meteorological records) the annual mean temperature (T_a) of the site. To develop the method, we computed equations (9) and (10) for 51 temperature conditions typical of archaeological sites where the mean annual temperatures ranged from 10 – 20°C, the seasonal variation ranged between 5 - 20°C, and diurnal variation ranged between 2 – 20°C. The activation energies assumed were 10,000 K for obsidian and 5,000 K for the cell. The key

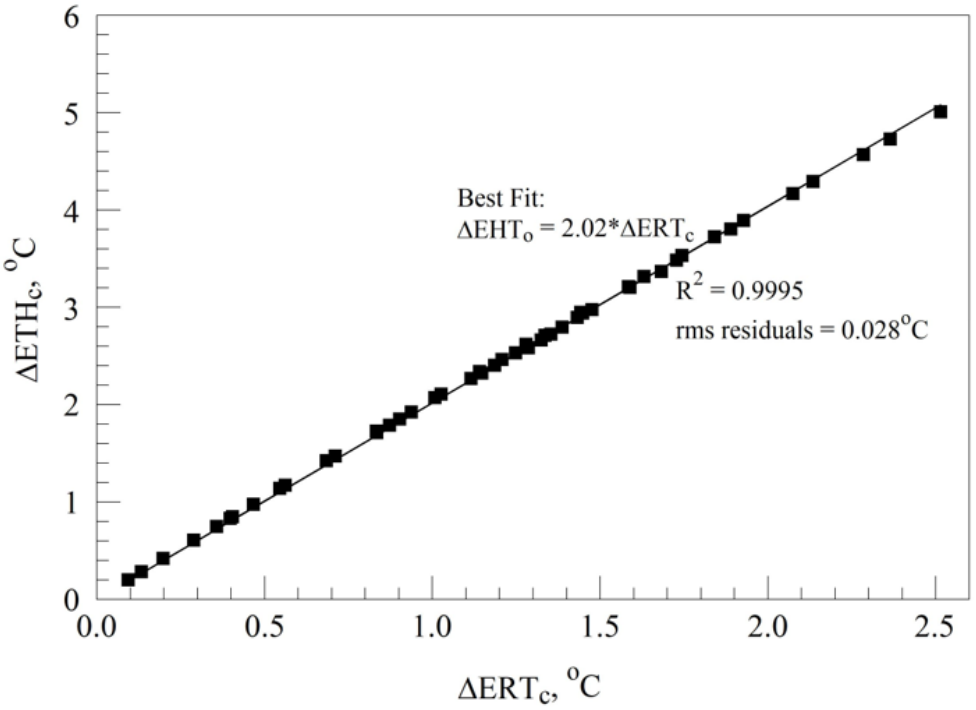

Figure 1. Adjustment of Ambrose/Trembour cell effective reaction temperature to obsidian effective hydration temperature.

parameter is the difference between the EHT (or ERT) and T_a, defined as:

$$\Delta T_c = ERT_c - T_a \quad (11a)$$

and

$$\Delta T_o = EHT_o - T_a \quad (11b)$$

Figure 1 shows a plot of ΔT_c (x-axis) vs. ΔT_o (y-axis). Visually the fit is very good, and the $R^2 = 0.9995$ with rms residuals of 0.028°C. The linear least squares best fit equation is:

$$\Delta T_o = 2.02*\Delta T_c \quad (12)$$

Thus, the best estimate of EHT for obsidian (EHT_o) based on ERT for an Ambrose/Trembour cell (ERT_c) and mean annual temperature (T_a) is:

$$EHT_o = T_a + 2.02*(ERT_c - T_a) \quad (13)$$

For a cell in most conditions of archaeological interest, this adjustment should give a correct EHT for obsidian which is precise to within 1°C, with negligible offset in the mean value.

The Pallmann Cell

The Pallmann cell is based on the conversion over time of an aqueous solution of sucrose to an invert sugar which is amixture of glucose and fructose. Polarized light passing through such a solution undergoes a rotation of the axis of polarization which increases with increasing invert sugar concentration. The reaction is temperature-sensitive and also sensitive to pH of the solution. The ERT equation for such a cell is similar to equation (7) above, with adjustment terms for pH of the solution (Norton and Friedman 1981:4), and equation (8) also applies to such a cell. The cells have been used for soil temperature measurements (Bai 2009; Friedman and Norton 1981; O'Brien 1971; Olmsted et al. 1981), and a precision in ERT of 0.25°C was

Parameter	Value
R_t	20°
R_∞	-20°
R_0	60°
Q	6029
Y	18.43
pH	3.1
Rotation angle accuracy	0.01°
pH accuracy	0.01

Table 2. Pallmann Cell Parameter Values

reported based on field tests (Norton and Friedman 1981:5). However, the laboratory processing of such a cell was more difficult that for the Ambrose/Trembour cell, and Pallmann cells were never widely used in archaeology.

Unlike the Ambrose/Trembour cell, the Pallmann cell is based on a chemical reaction which exhibits the Arrhenius dependence on temperature. The reaction is first-order, so the quantity of unreacted solution decays exponentially with time:

$$x = A*\exp(-k_1*t)$$

where: x is the number of unreacted moles of solution, A is the original number of moles, k_1 is the reaction rate, and t is time. If R_t is the rotation angle at time t, R_0 is the initial rotation angle, and R_∞ is the rotation angle at infinite time (asymptotic value), then A is proportional to $(R_\infty - R_0)$ and x is proportional to $(R_\infty - R_t)$, which yields after some algebra:

$$k_1 = \ln[(R_\infty-R_0)/(R_\infty-R_t)]/t \qquad (14a)$$

The reaction rate is catalyzed by H^+, so the logarithm of the overall reaction rate is:

$$\ln(k) = \ln(k_1) + pH \qquad (14b)$$

where: pH is the pH of the solution (O'Brien 1971). In practice, the values of R_0 and R_∞ are determined in the laboratory during the calibration process.

The reaction rate is a function of temperature by the Arrhenius equation (2), and the effective reaction temperature is:

$$ERT_c=-Q/[\ln\{\ln[(R_\infty-R_0)/(R_\infty-R_t)]/t\}+pH-Y] \quad (15)$$

Values for Y and Q have been reported to be Y ≈ 18.14 ± 0.87 and Q ≈ 5922 ± 111 Kelvins (Bai 2009: 31-32).

Measurement

The precision resulting from the measurement of optical rotation can be computed based on equations (14) and (15). Typical parameter values are in Table 2 (from Bai 2009). Assuming Y and Q are error-free, a simple Monte Carlo analysis, adding errors to the parameters in equation (15) and then computing ERT by equation (16) gives a precision in ERT of 0.13°C.

Calibration

The values for Y and Q are not error-free but are computed by a least-squares best fit to a calibration data set. Bai (2009:31-32) did not publish his calibration data set but did publish his results which are summarized in Table and compared with our Monte Carlo simulation results for the Ambrose/Trembour cell.

Cell	Activation energy, Kelvins	Y Intercept = ln(A_c)
Ambrose/Trembour cell	5416 ± 124, CV = 0.023	11.29 ± 0.40, CV = 0.035
Pallmann cell	5922 ± 111, CV = 0.018	18.14 ± 0.87, CV = 0.048

Table 3. Calibration Results

Our Monte Carlo simulation for the Ambrose/Trembour cell, discussed above, did account for error correlations, and yielded a standard deviation of ERT_c due to calibration of 0.295°C. As the parameters and their uncertainties are reasonably close for the two cases, we estimate the uncertainty in ERT_c due to calibration to be ≈ 0.295°C for the Pallmann cell as well. Combining this uncertainty with errors due to measurement (0.13°C) by a rms process yields a total uncertainty in ERT of 0.32°C, similar to the precision of the Ambrose/Trembour cell.

Activation Energy and Adjustment

This uncertainty of 0.32°C is for the ERT for the cell, and not for EHT of obsidian, since the activation energies differ. A Monte Carlo analysis similar to that for the Ambrose/Trembour cell, using Q = 6000 for the cell and Q = 10000 for obsidian, gives $EHT_o - ERT_c = 1.27 \pm 0.44$°C (10,000 iterations). The best estimate of EHT_o based on ERT_c and mean annual temperature (T_a) for the Pallmann cell is:

$$EHT_o = T_a + 1.68*(ERT_c - T_a) \qquad (16)$$

Once adjusted, the overall accuracy and precision of the Pallmann cell are similar to the Ambrose/Trembour cell where an EHT_o is within 1°C with negligible offset.

Dynamic EHT Computation

At the present time, the best fidelity in computing EHT is achieved by a dynamic model fed by a digital sensor, which involves applying equation (9) to digitally-recorded temperature data. A digital sensor-logger such as an Onset Corporation Hobo is placed at the site and set to record temperature hourly. (Digital sensor-logger cells are available with varying memory size, and it is important to estimate memory requirements before employing them. At least 64K is recommended). After one year the sensor is down-loaded into a computer in .csv format, which yields a time-series of the temperature noted as T(n) in equation (9) above. A simple program in MatLab or Python can be written to read the .csv file, convert to Kelvins by adding 273.15 to each recorded temperature, and carry out the computation in equation (9). Examples of this s method were demonstrated in Rogers (2008), using digitally-recorded temperature data for the years 2000 – 2005 from the Amargosa Desert Research Site near Beatty, NV, and by Franchetti et al. (2024) for Salamanca Cave, Argentina.

The accuracy achievable was estimated with a Monte Carlo simulation based on equation (9). The simulation adds random measurement errors to each temperature data point, with a standard deviation of 0.5°C, which it typical of digital sensors. The effects of uncertainty in activation energy are included by computing the error-free case based on an assumed value, and the case with temperature errors based on an actual value. The values of activation energy range between 9500 K and 10500 K, and statistics were computed after 10,000 iterations. We found the uncertainty in activation energy had a negligible effect over such a narrow range, so the resulting uncertainty of approximately 0.5°C, is entirely due to temperature measurement error.

Discussion and Conclusion

Based on this analysis we conclude that when uncertainties arising from the calibration

process of analog temperature cells are included, the effective reaction temperature experienced by the cell (ERT_c) is accurate to about 0.3°C. These conclusions apply to both the Ambrose/Trembour diffusion cell and the Pallmann chemical cell. However, this ERT_c is lower than the effective hydration temperature which would have been experienced by obsidian (EHT_o) exposed to the same temperature history, by between 1°C and 2°C. Therefore, an adjustment is necessary. The adjustment process differs slightly between the two types of cells, but either will yield an EHT_o with an uncertainty within 1°C. Each 1°C increase in EHT causes approximately an 11% increase in hydration rate, which in turn causes a 10% decrease in computed age, which facilitates adjusting the ages of previously published data.

A more accurate EHT, which avoids most of the issues with analog cells, is obtained by use of modern digital sensor-loggers, feeding a data stream directly to dynamic model of the hydration process, and yielding an accuracy of about 0.5°.

References Cited

Ambrose, Wallace. 1975. Intrinsic Hydration Rate Dating of Obsidian. In *Advances in Obsidian Glass Studies*, edited by R. E. Taylor, pp. 81–105. Noyes Press, Park Ridge, New Jersey.

Ambrose, Wallace. 1980. Monitoring Long-Term Temperature and Humidity. *AICCM Bulletin* 6(1):36–42.

Bai, Yan Ting. 2009. Distribution of Soil Temperature Regimes and Climate Change in the Mojave Desert Regions. Unpublished PhD dissertation, Department of Geosciences, University of California, Riverside.

Crank, J. 1975. *The Mathematics of Diffusion*. Oxford University Press, Oxford.

Doremus, R. H. 2002. *Diffusion of Reactive Molecules in Solids and Melts*. Wiley-Interscience, New York.

Franchetti, Fernando, Gustavo Neme, Adolfo Gil, M. Laura Salgan, Alexander K. Rogers, James Davenport, Raven Garvey, Olga Trofimova, Thegn N. Ladefoged, and Christopher M. Stevenson. 2024. Obsidian Hydration Dating by Infrared Transmission Spectroscopy. *Archaeometry* 66:1–18.

Friedman, Irving, and Daniel R. Norton. 1981. Ground Temperature Measurements near Yellowstone Park. Part III in *Ground Temperature Measurements*. Geological Survey Professional Paper 1203. U.S. Government Printing Office, Washington, D.C.

Friedman, Irving, and R. Smith. 1960. A New Method of Dating Using Obsidian: Part 1, the Development of the Method. *American Antiquity* 25(4):476–522.

Friedman, Irving, and William Long. 1976. Hydration Rate of Obsidian. *Science* 191(1):347–352.

Norton, Daniel R., and Irving Friedman. 1981. Pallmann Technique. Part I in *Ground Temperature Measurements*. Geological Survey Professional Paper 1203. U.S. Government Printing Office, Washington, D.C.

O'Brien, Phillip J. 1971. Pallmann Method for Mass Sampling of Soil, Water, or Air Temperatures. *Geological Society of America Bulletin* 82(10):2927–2932.

Olmsted, F. H., Irving Friedman, and Daniel R. Norton. 1981. Evaluation of the Pallmann Technique in Two Geothermal Areas of West-Central Nevada. Part II in *Ground Temperature Measurements*. Geological Survey Professional Paper 1203. U.S. Government Printing Office, Washington, D.C.

Rogers, Alexander K. 2008. Field Data Validation of an Algorithm for Computing Obsidian Effective Hydration Temperature. *Journal of Archaeological Science* 35:441–447.

Rogers, Alexander K., and Christopher M. Stevenson. 2017. Protocols for Laboratory Hydration of Obsidian, and Their Effect on Hydration Rate Accuracy: A Monte Carlo Simulation Study. *Journal of Archaeological Science: Reports* 16:117–126.

Stevenson, Christopher M., Alexander K. Rogers, Steven W. Novak, Wallace Ambrose, and Thegn N. Ladefoged. 2021. A Molecular Model for Obsidian Hydration Dating. *Journal of Archaeological Science: Reports* 36:102824.

Trembour, Fred W., and Irving Friedman. 1984. Present Status of Obsidian Hydration Dating. *Developments in Paleontology and Stratigraphy* 7.

Trembour, Fred W., Irving Friedman, F. Joseph Jurceka, and Franklin L. Smith. 1986. A Simple Device for Integrating Temperature, Relative Humidity, and Salinity over Time. *Journal of Atmospheric and Oceanic Technology* 3:186–190.

Trembour, Fred W., Franklin L. Smith, and Irving Friedman. 1988. Diffusion Cells for Integrating Temperature and Humidity over Long Periods of Time. *Materials Research Society Symposium Proceedings* 125:375–381.

ABOUT OUR WEB SITE

The IAOS maintains a website at http://www.deschutesmeridian.com/IAOS/ The site has some great resources available to the public, and our webmaster, Craig Skinner, continues to update the list of publications and must-have volumes.

You can now become a member online or renew your current IAOS membership using PayPal. Please take advantage of this opportunity to continue your support of the IAOS.

Other items on our website include:

- World obsidian source catalog
- Back issues of the *Bulletin.*
- An obsidian bibliography
- An obsidian laboratory directory
- Photos and maps of some source locations
- Links

Thanks to Craig Skinner for maintaining the website. Please check it out!

CALL FOR ARTICLES

Submissions of articles, short reports, abstracts, or announcements for inclusion in the *Bulletin* are always welcome. We accept submissions in MS Word. Tables should be submitted as Excel files and images as .jpg files. Please use the *American Antiquity* style guide for formatting references and bibliographies.

Submissions can also be emailed to the *Bulletin* at IAOS.Editor@gmail.com Please include the phrase "IAOS Bulletin" in the subject line. An acknowledgement email will be sent in reply, so if you do not hear from us, please email again and inquire.

Deadline for Issue #77 is December 1, 2026.

Email or mail submissions to:

Dr. Carolyn Dillian
IAOS Bulletin, Editor
Department of Cultures, Communities, and Environments
Coastal Carolina University
P.O. Box 261954
Conway, SC 29528
U.S.A.
IAOS.Editor@gmail.com

Inquiries, suggestions, and comments about the *Bulletin* can be sent to IAOS.Editor@gmail.com Please send updated address/email information to Lucas Martindale Johnson at lucas.r.m.johnson@gmail.com.

MEMBERSHIP

The IAOS needs membership to ensure success of the organization. To be included as a member and receive all of the benefits thereof, you may apply for membership in one of the following categories:

Regular Member: $20/year*
Student Member: $10/year or FREE with submission of a paper to the *Bulletin* for publication. Please provide copy of current student identification.
Lifetime Member: $200

Regular Members are individuals or institutions who are interested in obsidian studies, and who wish to support the goals of the IAOS. Regular members will receive any general mailings; announcements of meetings, conferences, and symposia; the *Bulletin*; and papers distributed by the IAOS during the year. Regular members are entitled to vote for officers.

*Membership fees may be reduced and/or waived in cases of financial hardship or difficulty in paying in foreign currency. Please contact the Secretary-Treasurer with a short explanation regarding lack of payment.

NOTE: The IAOS asks that all payments be made using the PayPal link on our website: http://www.deschutesmeridian.com/IAOS/membership.html

For more information about membership in the IAOS, contact our Secretary-Treasurer:

Lucas Martindale Johnson
lucas.r.m.johnson@gmail.com.

Membership inquiries, address changes, or payment questions can also be emailed to lucas.r.m.johnson@gmail.com.

ABOUT THE IAOS

The International Association for Obsidian Studies (IAOS) was formed in 1989 to provide a forum for obsidian researchers throughout the world. Major interest areas include: obsidian hydration dating, obsidian and materials characterization ("sourcing"), geoarchaeological obsidian studies, obsidian and lithic technology, and the prehistoric procurement and utilization of obsidian. In addition to disseminating information about advances in obsidian research to archaeologists and other interested parties, the IAOS was also established to:

1. Develop standards for analytic procedures and ensure inter-laboratory comparability.
2. Develop standards for recording and reporting obsidian hydration and characterization results
3. Provide technical support in the form of training and workshops for those wanting to develop their expertise in the field.
4. Provide a central source of information regarding the advances in obsidian studies and the analytic capabilities of various laboratories and institutions

NATIONAL ACADEMY OF SCIENCES OF REPUBLIC OF ARMENIA

INSTITUTE OF GEOLOGICAL SCIENCES

INSTITUTE OF ARCHAEOLOGY AND ETHNOGRAPHY

THE SECOND CIRCULAR

INTERNATIONAL OBSIDIAN CONFERENCE IOC–2026

FROM MAGMA TO ARTIFACT: THE GEOLOGY AND ARCHAEOLOGY OF OBSIDIAN

Yerevan, Armenia, 28 September – 01 October, 2026

Obsidian Hearth, sculpture by Jean-Michel Othoniel (b. 1964), France, 2014, Boghossian Foundation Collection, Lovers Park, Yerevan, 143x200x220 cm.

IOC SCIENTIFIC COMMITTEE

Katalin T. Biró — Hungarian National Museum, Budapest, Hungary
Kyle P. Freund — Far Western Anthropological Research Group, INC, CA, USA
Ellery Frahm — Yale University, New Heaven, CT, USA
Michael D. Glascock — University of Missouri, Columbia, MO, USA
Yaroslav V. Kuzmin — Institute of Geology & Mineralogy, Siberian Branch of the Russian Academy of Sciences, Novosibirsk, Russia
François-Xavier Le Bourdonnec — University Bordeaux Montaigne, Pessac, France
András Markó — University of Szeged, Szeged, Hungary
Theodora Moutsiou — University of Cyprus, Nicosia, Cyprus
Akira Ono — Professor Emeritus, Tokyo Metropolitan University, Tokyo, Japan
Yoshimitsu Suda — Nagasaki University, Nagasaki, Japan
Robin Torrence — Australian Museum, Sydney, Australia
Robert Tykot — University of South Florida, Tampa, FL, USA
Andrea Vianello — University of South Florida, Tampa, FL, USA

LOCAL ORGANIZING COMMITTEE

Khachatur Meliksetian (General Chair) - Institute of Geological Sciences, Armenia
Arsen Bobokhyan (Program Chair) - Institute of Archaeology and Ethnography, Armenia
Ruben Badalyan (Program Chair) - Institute of Archaeology and Ethnography, Armenia
Pavel Avetisyan (Publication Chair) - Institute of Archaeology and Ethnography, Armenia
Lilit Sahakyan (Poster Session Chair) - Institute of Geological Sciences, Armenia
Boris Gasparyan (Excursion Chair) - Institute of Archaeology and Ethnography, Armenia
Natella Aghamalyan (Logistic Chair) - Institute for Physical Research, Armenia
Seda Avagyan-- Institute of Geological Sciences, Armenia
Edmond Grigoryan - Institute of Geological Sciences, Armenia
Tatevik Boyakhchyan - Institute of Geological Sciences, Armenia

LOCAL ORGANIZING COMMITTEE CONTACTS

Conference Web-site www.ioc2026.geology.am
e-mail: IOC2026@geology.am
Payment: Registration fees can be paid conference web site (payments will be open April 2026)
Telephones/WhatsApp : +374 94775980, +374 91503175 , +374 91308431

CONFERENCE TOPICS

- **Petrology and geochemistry of obsidians**
- **Volcanic processes and physical properties of rhyolite melts**
- **Provenance studies of archaeological obsidian: source exploitation and raw material distribution**
- **Typological, technological, and use-wear analysis of archaeological obsidian**
- **History and methods of provenance studies in archaeology**

Abstracts volume with ISBN and DOI will be printed and distributed over conference web-site

CONFERENCE VENUE

ROUND HALL OF THE PRESIDIUM OF ARMENIAN NATIONAL ACADEMY OF SCIENCES

VISA INFORMATION

- ✓ ***Citizens of all European Union countries, Switzerland, UK, the USA, China, Iran, Japan, Brazil, Argentina and the states of former USSR republics do not need visas to enter Armenia.***
- ✓ ***Citizens of many countries can easily get visa on arrival at the Yerevan Zvartnots international airport (visa fee is ~ USD 6).***
- ✓ ***Citizens of some countries are required to apply for visa beforehand***

For more information about the visa policy of Armenia, please check the regularly updated websites:
http://mfa.am/en/visa/
https://en.wikipedia.org/wiki/Visa_policy_of_Armenia

AIRPORT INFORMATION

The new terminal of Yerevan Zvartnots International Airport was built in 2013. Currently more than 30 airlines operate flights to and from Yerevan, totally about 40 flights per day from/to Europe, Asia, Russia and the Middle East. Among them: Air Armenia, Air France, FlyOne, Lufthansa group/Austrian Airlines, Qatar Airways, Aeroflot, S7 Airlines, China Southern Airlines, Lot Polish Airlines, Air Arabia, Aegean Airlines, Brussels Airlines, WizzAir and others.

Airport website: www.zvartnots.aero

HOTELS IN YEREVAN

A large selection of hotels is available in Yerevan – from luxury to affordable.




BACKGROUND: OBSIDIAN OCCURENCES IN ARMENIA

Evidence of the Quaternary and Holocene volcanism in Armenia include plateau-basalt lavas, several large stratovolcanoes (e.g. Aragats) and associated ignimbrites. In Armenia, there are more than 500 Quaternary–Holocene monogenetic volcanoes located in several volcanic fields/highlands and forming one of the densest volcano clusters on the Earth. Compositionally, Armenian Quaternary magmas range from picrobasalts and basanites to rhyolites, and reveal unique geochemical fingerprints of collision zone volcanism that differ from those at island arcs, continental intraplate/oceanic islands settings and mid-ocean ridges. Armenia, with its extensive Pliocene–Quaternary volcanism, hosts high-quality obsidian in five volcanic provinces. Many sources are accessible and show archaeological evidence of prehistoric use. Obsidian was a valuable raw material in prehistoric times across the Caucasus, Near East, and Mediterranean, often found far from its geological sources. Its geochemical properties enable precise provenance tracing, shedding light on ancient trade routes and regional resource utilization. Unlike metals, obsidian retains its composition during tool production, and its distinct geochemical signatures allow clear source differentiation.

Distribution of obsidian sources in Armenia, Georgia and Eastern Turkey (after Meliksetian et al., 2024).

CONFERENCE SCHEDULE

DATES: 28 September – 01 October 2026

CONFERENCE FORMAT

The conference format will be onsite.

Abstract submission deadline: May 15, 2026

REGISTRATION FEES

Onsite regular participants – 200,000.00 Armenian drams (~500 USD)

Onsite student participants 100,000.00 Armenian drams (~250 USD)

Accompanying persons - 100,000.00 Armenian drams (~250 USD)

Online (Remote) participants – 20,000.00 Armenian drams (~50 USD)

Payment on site will be possible, but an additional fee of 50 USD will be charged.

The Registration fee includes:

- ***Attendance at the scientific sessions***
- ***Coffee breaks and lunches during the meeting***
- ***Printed abstracts volume and excursion guide***
- ***Transportation and lunch during two mid-conference field trips***
- ***Conference banquet***
- ***Conference materials and an obsidian souvenir***
- ***Guided tour to the History Museum of Armenia***
- ***Welcome "Icebreaker" event***
- ***Special sightseeing travel program will be offered to the registered accompanying persons***

The registration fee refunds will be available up to one month prior to the conference.

The registration fees do not include the costs of international travel and accommodation in Yerevan.

Abstracts should be prepared in the following format:

Font: Times New Roman, 12 pt

Line spacing: 1.5

Margins: 2.5 cm on all sides

Maximum length: 400 words

Include title, authors, affiliation, and email

Indicate preferred presentation type via email (oral or poster)
Please submit your abstract in Word to IOC2026@geology.am

GUIDED TOUR TO THE HISTORY MUSEUM OF ARMENIA

The History Museum of Armenia is a nationally significant cultural institution dedicated to preserving and showcasing Armenia's heritage. With a collection of over several hundreds of artifacts spanning from Paleolithic times to today, the museum serves as a bridge between the past and the future, contributing to science, education, and tourism.

Obsidian nuclei (Neolithic, VI Mil. BC) in the museum exhibition

Exhibition of History Museum of Armenia

Exhibition of History Museum of Armenia

MID CONFERENCE FIELD TRIP 1: ONE DAY, INCLUDING ARTENI OBSIDIAN SOURCE AND BAROZH-12 MIDDLE PALEOLITHIC SITE

Arteni rhyolite (obsidian) volcano

Arteni volcanic complex is located within Aragats volcanic province. The age of Arteni rhyolites considered to be Early Pleistocene; K-Ar ages are: for Mets Arteni 1.45–1.5 Ma (Chernishev et al., 2002); fission track ages –1.27 Ma (Oddone et al., 2000) and 1.26 Ma

for Pokr Arteni (Lebedev et al., 2011). Thus, rhyolitic eruptions and the formation of domes of Arteni volcano correspond to the Early Pleistocene. Eruption products of Arteni volcano are covered by more recentMiddle Pleistocene andesitic lava flows of neighboring Ddmasar cinder cone and ignimbrites of Aragats stratovolcano.

Arteni is the most compound rhyolitic volcanic complex in Armenia, and it consists of two independent rhyolitic volcanoes: Mets (Big) and Pokr (Little) Arteni (2047 and 1754 m asl, respectively). Volcanic activity began with an eruption of perlite-pumice pyroclastics, followed by eruptions of detrital perlite and zonal obsidian that flowed westward and southward; shorter flows also went northward. Arteni obsidian is of high quality; "smoky quartz" of the translucent, reddish-brown, black, and other varieties are known.

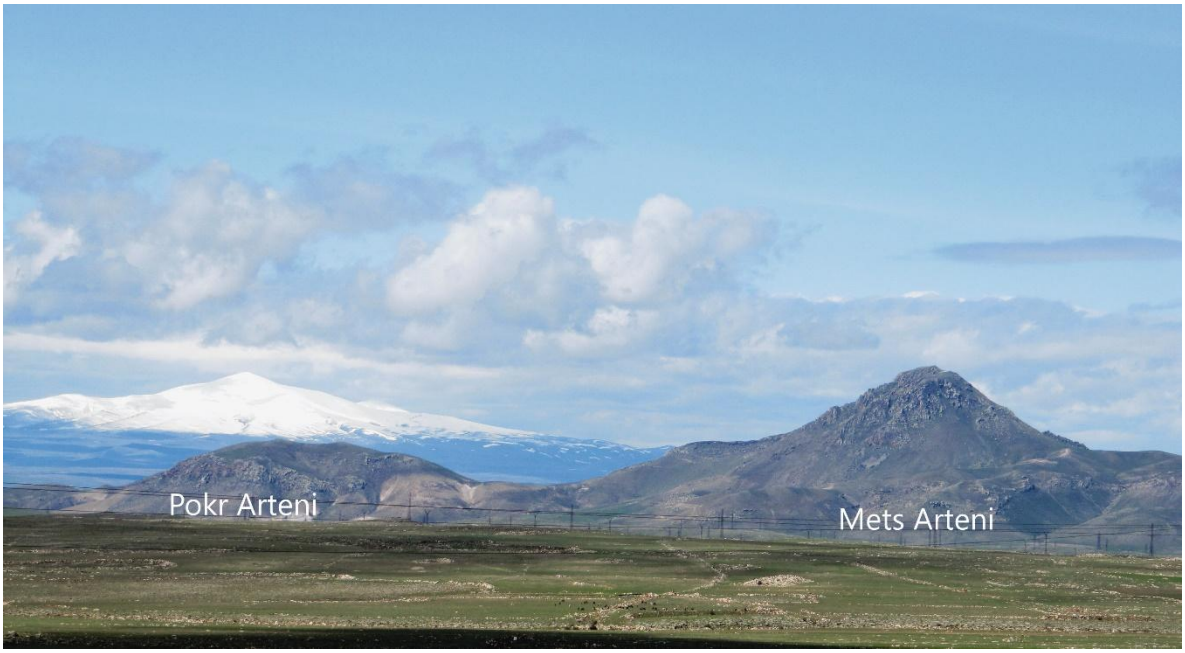

Arteni volcanic complex in Armenia, Aragats volcanic province.

Products of explosive eruptions of rhyolite pumice and perlite pyroclastics (left). Obsidian cliff in small modern quarry across a lava flow erupted from Pokr Arteni volcano(right).

Barozh-12, Middle Paleolithic open-air site and obsidian workshop

Located in western Armenia, at the edge of the Ararat Depression near the Mt Arteni volcano (Fig. 1.16), the open-air Middle Paleolithic site of Barozh-12 was excavated by an international–Armenian archaeological team from 2009 – 2014 (Glauberman et al., 2020a,b). This site yielded significant data on Late Middle Paleolithic technology, land use, and hominin behavior in a region that has heretofore been little explored. The lithic assemblage (Fig. 1.17) appears similar to those from other contemporaneous Middle Paleolithic sites in the region, and luminescence age estimates indicate the site was occupied around 60 – 31 ka, the time range when archaic and anatomically modern humans may have overlapped temporally and/or geographically. Barozh-12 is a large, high-density Middle Paleolithic site. A total of 4.85 m^3 of excavated sediments yielded 17,317 obsidian artifacts with densities ranging from 1600–5200 artifacts / m^3 according to stratigraphic unit.

Unidirectional-convergent and unidirectional Levallois core reduction techniques dominate in the core and flake assemblage, and retouched pieces are numerous. These are mainly retouched Levallois points and convergent and other unifacial scraper forms on Levallois blanks (Fig. 1.17).

View of Barozh-12 open-air Paleolithic site and test trench. Arteni volcano is in the background.

Surface and excavated artifacts are of all size classes and technological categories, including tool re-sharpening flakes and core trimming elements. Artifacts class frequencies and cortex analysis also suggest that all stages of core reduction and tool use, maintenance and discard occurred on site. While artifact assemblage analysis also reveals that site occupation intensity varied over time at the site.
The extent of a 'raw material exploitation territory' is suggested by obsidian sourcing. Results of portable X-Ray fluorescence (pXRF) analysis of samples of obsidian artifacts from all strata (n = 318) indicate that most were manufactured from local (1 – 2 km) Pokr and Mets Arteni material, while a smaller number of mainly retouched artifacts were manufactured on material that originates between 40 and 190 linear km away. Artifact transports overlap with sources in the Armenian Highlands and eastern Anatolia, and other Middle Paleolithic sites within the same time range. Interestingly, obsidian sourcing at the Upper Paleolithic site of Aghitu-3, around 200 km to the south of Barozh-12 also shows exploitation of the same obsidian sources. This suggests overlapping mobility ranges of hominins that employed both Middle and Upper Paleolithic technologies in the region starting around 40 ka.

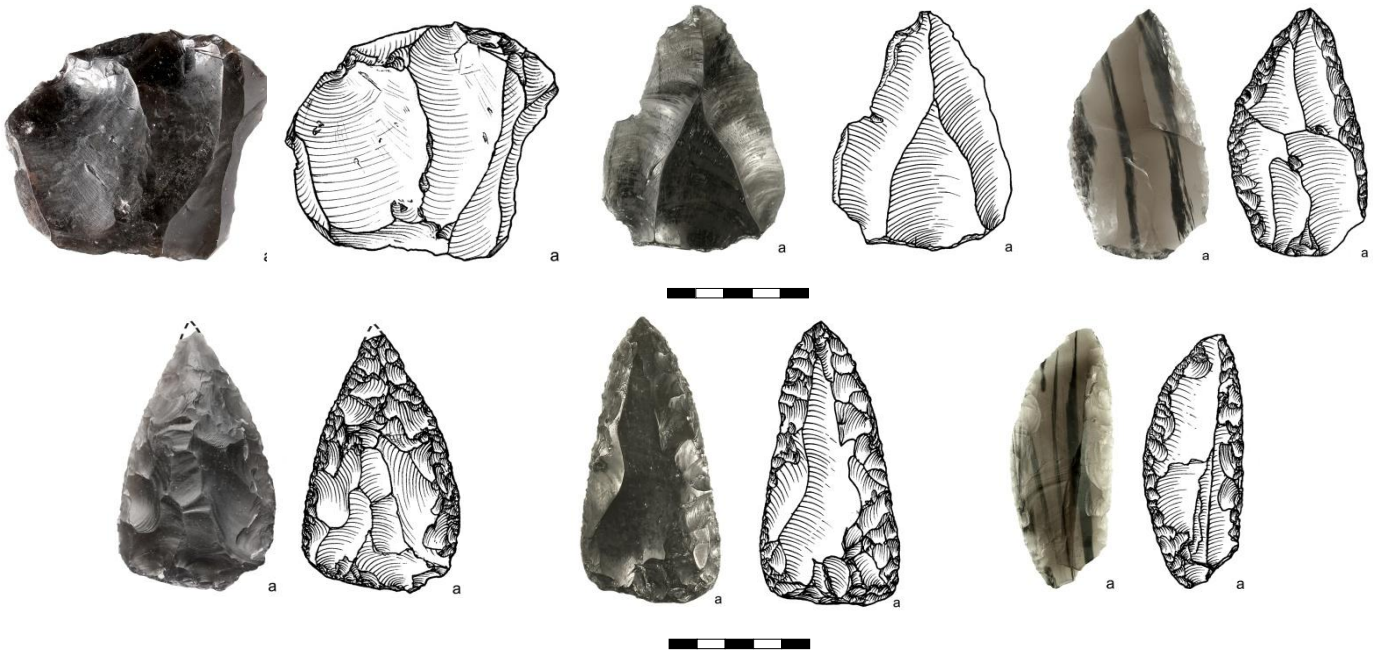

Selected artifacts from Barozh-12: 1 Levallois core; 2 Levallois point; 3 Double straight-convex scraper; 4 Mousterian point; 5 Convergent scraper; 6 Double straight-convex scraper (modified after Glauberman et al. 2020a)

MID-CONFERENCE FIELD TRIP 2: GARNI HELLENISTIC TEMPLE, COLUMNAR JOINTS LAVA FLOW, GEGHARD MONASTERY, GUTASNAR OBSIDIAN SOURCE

Garni and Geghard

a. Visit to 1st century AD Classical Hellenistic temple of Garni.
b. Visit to gorge of Azat River, spectacular columnar joints lava flow and Garni active fault.
c. Visit to 4th – 13th Century AD Geghard monastery and view of Voghjaberd volcanoclastic suite of Upper Miocene – Pliocene age.
d. Gutansar volcano and obsidian outcrops

Garni Hellenistic temple

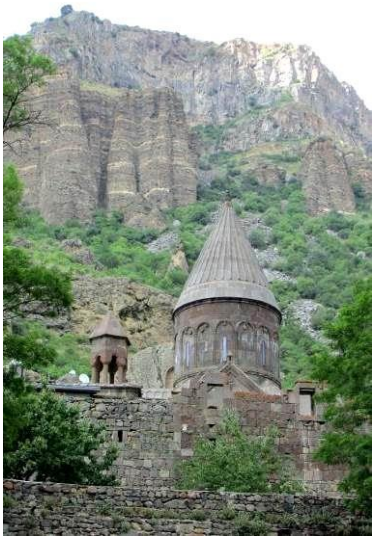

Geghard Monastery

Columnar joint lava flow in Garni, 127 ka,

Jraber extrusive body related to the Gutansar volcanic complex.
Obsidian outcrop on the Yerevan-Sevan highway

References

Glauberman, P., Gasparyan, B., Wilkinson, K., Frahm, E., Nahapetyan, S., Arakelyan, D., Raczynski-Henk, Y., Haydosyan, H., Adler, D.S., 2020a. Late Middle Paleolithic technological organization and behavior at the open-air site of Barozh 12 (Armenia). *Journal of Paleolithic Archaeology* 3, 1095-1148.

Glauberman, P.J., Gasparyan, B., Sherriff, J., Wilkinson, K., Li, B., Knul, M., Brittingham, A., Hren, M.T., Arakelyan, D., Raczynski-Henk, Y., Nahapetyan, S., Haydosyan, H., Adler, D.S., 2020b. Barozh 12: formation processes of a late Middle Paleolithic open-air site in western Armenia. *Quaternary Science Reviews* 236, 106276, 1-23.

Meliksetian, K., Pernicka, E., Badalyan, R., Schifer, T., Keller, J., Gasparyan, B., Jrbashyan, R., Navasardyan, G., Kunze, R., (2024) Trace Element Geochemistry of Armenian Obsidian Sources and the Provenance of Archaeological Obsidian Artefacts. in Strategies of Obsidian Procurement, Knapping and Use in the First Farming Societies Vinet, A., Guilbeau, D., Milić, B (Eds.). Verlag der Österreichischen Akademie der Wissenschaften. Pp 167-249 https://doi.org/10.1553/978OEAW93241

Chernishev, I.V., Lebedev, V.A., Arakelyants, M.M., Jrbashyan, R.T., Ghukasyan, Y.G., (2002). Quaternary geochronology of the Aragats volcanic centre, Armenia: evidence from K–Ar dating. Doklady Earth Sciences, 384, 95–102 (in Russian).

Oddone, M. Bigazzi, G. Keheyan, Y. Meloni S. 2000. Characterisation of Armenian obsidians: Implications for raw material supply for prehistoric artifacts. Journal of Radioanalytical and Nuclear Chemistry 243,3, 2000, 673-682.

Lebedev, V.A., Chernyshev, I.V., Yakushev, A.I. 2011. Initial time and duration of Quaternary magmatism in the Aragats neovolcanic area (Lesser Caucasus, Armenia). Doklady Earth Sciences, 437, 2011, 532-536.